

Focused Ion Beam Recovery of Hypervelocity Impact Residue in Experimental Craters on Metallic Foils.

G.A. Graham¹, N. Teslich², Z.R. Dai², J.P. Bradley¹,
A.T. Kearsley³ and F. Hörz⁴

¹Institute of Geophysics and Planetary Physics, Lawrence Livermore National Laboratory, Livermore, CA 94551, USA.

²Chemistry and Material Sciences, Lawrence Livermore National Laboratory, CA 94551, USA.

³Department of Mineralogy, The Natural History Museum, London, SW7 5BD, UK.

⁴Astromaterials Research Office, NASA Johnson Space Center, Houston, TX 77058, USA.

Corresponding Author:

Dr. Giles Graham

Institute of Geophysics & Planetary Physics

Lawrence Livermore National Laboratory

7000 East Avenue, L-413

Livermore

CA 94551

USA

Tel: +1-925-423-5523

Fax: +1-925-423-5733

Email: graham42@llnl.gov

Total no. Of Words: 4284

Figures: 4

Submitted to
Meteoritics & Planetary Science
as a short report paper

Abstract:

The Stardust sample return capsule will return to Earth in January 2006 with primitive debris collected from Comet 81P/Wild-2 during the fly-by encounter in 2004. In addition to the cometary particles embedded in low-density silica aerogel, there will be micro-craters preserved in the Al foils (1100 series; 100 μm thick) that are wrapped around the sample tray assembly. Soda lime spheres ($\sim 49 \mu\text{m}$ in diameter) have been accelerated with a light-gas-gun into flight-grade Al foils at 6.35 km s^{-1} to simulate the potential capture of cometary debris. The preserved crater penetrations have been analyzed using scanning electron microscopy (SEM) and x-ray energy dispersive spectroscopy (EDX) to locate and characterize remnants of the projectile material remaining within the craters. In addition, ion beam induced secondary electron imaging has proven particularly useful in identifying areas within the craters that contain residue material. Finally, high-precision focused ion beam (FIB) milling has been used to isolate and then extract an individual melt residue droplet from the interior wall of an impact penetration. This enabled further detailed elemental characterization, free from the background contamination of the Al foil substrate. The ability to recover “pure” melt residues using FIB will significantly extend the interpretations of the residue chemistry preserved in the Al foils returned by Stardust.

Introduction:

The study of comets is fundamental in understanding early solar system processes (e.g. Brownlee, 2003; Hanner, 2003). To date, much of the knowledge gained on the composition of specific comets is from remote or in-situ analysis (e.g. Kissel et al., 1986; Kissel et al., 2004). Yet the most definitive characterization can only really be achieved utilizing the diverse range of analytical instruments currently available in the laboratory (Zolensky et al., 2000). Some interplanetary dust particles (IDPs) have already been linked to cometary sources based on mineralogical and optical spectroscopy properties (Bradley and Brownlee, 1986; Bradley et al., 1999). However, it has not proven possible to define a specific parent body source.

In January 2004, the successful fly-by of NASA's Stardust spacecraft with comet 81P/Wild-2 resulted in the capture of abundant cometary debris (Brownlee et al., 2004; Tuzzolino et al., 2004). In addition to the primary mission goal of the comet fly-by, the reverse-side of sample tray assembly (STA) was exposed to an interstellar dust stream during parts of the outbound cruise phase (Brownlee et al., 2003). The cometary and interstellar dust particles were primarily captured in low-density, highly porous silica aerogel tiles (Tsou et al., 2003). As a result, a number of papers have dealt with the technique issues of material recovery from deep penetration tracks in aerogel generated by laboratory simulations or by low-Earth orbit (LEO) space exposure, to prepare for Stardust's return (e.g. Graham et al., 2004; Westphal et al., 2004; Ishii et al., 2005a and 2005b).

The STA that holds the individual aerogel tiles is wrapped with 100 μm thick Al foils (1100 series). The space-exposed surfaces of these foils will also retain a record of the

hypervelocity encounters with both interstellar and cometary particle populations. Previous studies of metallic surfaces exposed in space, e.g. those from the Long Duration Exposure Facility (LDEF), showed evidence of micrometer-sized craters as a result of meteoroid or orbital debris collisions (e.g. Bernhard et al., 1993). From analysis of impact residue chemistry preserved within the craters it was possible to derive the original impactor composition (e.g. Bernhard et al., 1993; Brownlee et al., 1993). In addition to SEM/EDX studies, novel replication and residue recovery techniques enabled detailed TEM studies of the meteoroid debris (Teetsov and Bradley, 1986; Bradley et al., 1986; Brownlee et al., 1993). These techniques will be employed on the Stardust foil samples. However, it is important to explore the new analytical capabilities that are now available for careful selection, preparation and manipulation of specifically located micrometer-sized material. Here we report on the use of focused ion beam microscopy to extract residue material from an impact preserved in Al foils to simulate potential Stardust recovery.

Methods:

Light-Gas-Gun Simulations

A number of metallic foils that have previously been exposed in low-Earth-orbit (LEO) as part of either dedicated experiments (such as those on LDEF) or as target-of-opportunity (e.g. on the Solar Maximum satellite) could have been used to develop and test capabilities for recovery and analysis of impacted material (e.g. Bradley et al., 1986; Bernhard et al., 1993). As meteoroid impacts on space-exposed surfaces are likely to have occurred at velocities between 10-20 km s⁻¹ (e.g. Brownlee et al., 1993), they are not

a representative analogue for the Stardust encounter velocity of $\sim 6 \text{ km s}^{-1}$. As a result, a comprehensive shot program was set-up to provide analogous materials for laboratory investigation to support interpretation of Stardust samples.

The laboratory simulation experiments described in this paper were performed using the small caliber (5 mm bore) 2-stage Light Gas Gun (LGG) at the Johnson Space Center (JSC), Houston. Glass spheres, of known size range (Kearsley et al., this volume), and meteoritic materials (e.g. crushed Allende) were used as projectiles for calibration studies. Rather than accelerate individual particles, a “shot gun” approach is utilized by loading multiple projectiles into the small, central cavity of a 4-piece, serrated sabot. By design, the 4 sabot quadrants separate radially during free flight, yet they allow a substantial fraction of the projectile ensemble to remain on straight trajectories and to ultimately reach the target site.

The LGG at JSC is fitted with a number of flapper valves, mechanical apertures, and a sabot catcher system that minimize the contamination so that only those projectiles that reside within < 1 degree of the gun axis will make it on target. For these experiments the target material used was Stardust flight-grade $\sim 100 \text{ }\mu\text{m}$ thick Al foil (1100 series) supplied to JSC by Peter Tsou (NASA/JPL). For each of the shots the foils were wrapped around a $25 \times 25 \times 3.12 \text{ mm}$ Al (6061, T6 series) plate, the latter simulating the Stardust collector frame.

The impact penetrations and residue material that are discussed in this paper are from JSC shot #2382, a shot that accelerated soda lime glass spheres ($43\text{-}54 \text{ }\mu\text{m}$ in diameter) into the Al-foil target at 6.35 km s^{-1} . The velocity was measured using laser occultation methods and IR photo diodes for determination of the sabot pieces. Additionally,

velocity of projectiles impacting the foil was measured using an impact flash detector. Typically, sabot velocity and projectile velocity agree to better than 1%.

Imaging & Microanalysis

The foil target from JSC shot #2382 was initially imaged using a Leica MZ16 stereomicroscope fitted with a Leica DC500 12 mega-pixel CCD camera. The entire foil (25x25 mm) was attached to a large diameter pin-stub using conductive carbon paint. It was then imaged, analyzed and subjected to precision ion milling using an FEI Nova 600 dual beam microscope comprising of a Ga⁺ liquid metal source focused ion beam (FIB) and field emission gun scanning electron microscope (FESEM). The dual beam microscope was fitted with an EDAX Genesis energy dispersive X-ray (EDX) spectrometer and an OmniprobeTM tungsten needle nanomanipulator. The secondary electron imaging was performed at 5 kV with a beam current of 0.15 nA and the EDX single-point spot analysis and mapping were performed at 15 – 20 kV with a beam current of 0.26 nA. The FIB imaging and milling was carried out at 30 kV with a beam current ranging from 30 – 1000 pA. Imaging and elemental analysis of extracted residue were performed using 200 kV FEI Tecnai G2 F20 UT (scanning) transmission electron microscope fitted with an EDAX EDX spectrometer and FEI TIA spectral processing software.

Results

SEM/EDX Imaging and Analysis

From the secondary electron imaging of the foil target, we determined that the crater

diameters ranged from 214 μm to 223 μm (Fig. 1a). The impact craters studied had completely penetrated the 100 μm 1100 series foil and terminated in the 6061 Al plate. As a result the observed impacts have steep sidewalls and flat bottom morphologies (Fig. 1a and 2a). The reduction in the cratering efficiency as a result of the shock reverberation of the foil and plate leads to lower crater diameters than the predicted value ($\sim 236\mu\text{m}$ crater diameter) from the calibration plot by Kearsley et al. (this volume). The impact residue morphologies observed within the craters varied from thin films to vesicular glass. They are typical for those generated by Si-rich materials and are similar to those observed in LDEF craters generated by silicate-dominated meteoroids (e.g. Bernhard et al., 1993; Brownlee et al., 1993).

In addition to acquiring crater diameters to assist confirmation of the original particle flux estimations of the Stardust encounter (Tuzzolino et al., 2004), the craters will also contain remnants of the comet Wild-2 debris. A particularly useful technique for identifying residue material within craters is EDX analysis using either a single spot (e.g. Bernhard et al., 1993) or elemental mapping mode (e.g. Graham et al., 2001). Both of these approaches were used to analyze the residue material generated by the soda-lime projectiles (Fig 1b-e). As the impacts have penetrated into the 6061 Al plate, the melt residue composition may be a complex mixture of the foil and plate substrates as well as the remnants of the soda lime projectiles.

FIB Imaging

The traditional method for surveying and subsequent identification of impact craters on metallic surfaces is SEM imaging using secondary electron and back-scattered electron

image modes. Back-scattered electron imaging (BEI) has proven particularly useful where there is substantial compositional contrast between a projectile residue and the impacted substrate, such as sulfide residues on borosilicate glass (e.g. Kearsley et al., 2005). It is, however, less effective when there is little inherent contrast, such as between silicate impactor residue and solar cell glass. In craters on aluminium foils, the compositional contrast in BEI might be expected to reveal residue easily. Unfortunately, the complex fine-scale crater topography masks much of the desired contrast.

Ion-induced secondary electron images can be acquired using the FIB (Phaneuf, 2004). Potentially, there is increase in the material contrast that can be observed in FIB-secondary electron images compared to conventional SEM secondary and back-scattered electron images. Figure 2 shows a conventional secondary electron image, and a FIB-secondary electron image with clear compositional difference between the impact residue and the substrate visible in the latter. Unlike conventional secondary electron imaging, FIB imaging is a destructive technique as the interaction between the Ga⁺ ions and the substrate will result in the removal of material and the implantation of Ga. However at the low beam current (30 pA) used in this study, the loss of material from the FIB imaging was negligible. Ga implantation may interfere with EDX analysis of Na (there are major overlaps between the relatively broad peaks of Ga-L and Na-K X-ray lines), but is unlikely to compromise other methods of analysis.

Residue Extraction using FIB

FIB microscopy has now become a well-established technique in materials science, especially for preparing site-specific electron transparent sections from bulk materials

(e.g. Phaneuf, 2004). For detailed elemental and isotopic studies of the cometary impact residue deposited in Al foil craters, it is important that the material can be recovered. Depending on the size of the craters and the distribution of the residue within the craters, there are two approaches that can be utilized using FIB. For small craters, typically 10-15 μm in diameter, it is possible to prepare complete TEM cross-sections of the entire crater that contain both the residue and the substrate (see Leroux et al., this volume for an in-depth discussion of this methodology). Complete cross-sections work extremely well when the residue is deposited as a film over most of the interior surface of the crater. However as was shown in LDEF studies, the deposition of residue material within craters is highly varied, ranging from thin-films, to more massive melt-liners and isolated melt beads/droplets, and may even include unmelted fragments of projectile material (Brownlee et al., 1993). Therefore, the second approach utilizing FIB, is to recover isolated residue material from within a crater. Figure 3a and 3b shows an impact that contains a micrometer-sized droplet (approximately 7 μm x 11.5 μm) in addition to the typical thin film of melt residue. Normally, a protective 2-3 μm thick layer of Pt is deposited on the top surface of the material that is going to be subjected to ion milling, as the initial process can result in ion beam damage up to a depth of 10 nm within the surface of interest. As the melt droplet in Figure 3 was the product of extreme alteration to the original projectile material (during the hypervelocity capture), it was considered that protection by deposition of Pt was unnecessary. The FIB was initially used to remove material from the interface between the droplet and the wall of the foil (Fig. 3c) with a beam current of 1000 pA and 30 kV accelerating voltage. To ensure that the droplet did not fall into the crater pit, a small Pt “strap” was deposited from the droplet to

the crater wall. The tip of the OmniprobeTM tungsten needle was attached to the outer surface of the droplet using Pt, after which the FIB was used to remove the remaining interface material and the Pt “strap”, at a reduced 300 pA beam current at 30 kV. This enabled the bulk of the droplet to be extracted from the wall of the crater (Fig. 3d). Within the chamber of the dual beam microscope, the OmniprobeTM tungsten needle was moved over to the TEM grid holder and the droplet was attached to the arm of one of the copper grids using Pt. The needle-droplet interface was removed using the FIB, leaving the droplet attached to the TEM grid (Fig. 3e). The droplet was then thinned to electron transparency (~100 nm thick) using the 30 kV FIB at 300 and then 100pA beam current (Fig. 3f).

Discussion

The hypervelocity capture of cosmic dust particles results in varying degrees of alteration. Meteoritic silicate melt glasses were frequently observed lining the walls of the LDEF craters (Bernhard et al., 1993; Brownlee et al., 1993). Therefore it might be argued that alteration of the original crystallographic structure during hypervelocity capture severely limits use of cometary impact residues in understanding the mineralogical composition of the comet. However it is noteworthy that, in addition to the melt glasses, some LDEF craters contained well-preserved mineral grains, some even containing solar flare tracks (Brownlee et al., 1993). We conclude that it is important to demonstrate a capability to recover cometary material from the craters. For LDEF craters and previous LEO retrieved materials (e.g. the thermal blanket from the Solar Maximum satellite), the impact residues were recovered from the substrates using micro-replication

and ultramicrotomy techniques (Teetsov and Bradley, 1986; Bradley et al., 1986). Although these techniques were successful in the recovery of meteoroid material (e.g. Brownlee et al., 1993), their methodology requires high skill levels and is time-consuming and can result in the loss of material. FIB methodology requires equal skill and is also time-consuming depending on the size of the structure to be ion milled. The significant advantage of the FIB methodology is the ability for controlled site-specific recovery of residue material from a crater. Furthermore, the microtomed sections prepared from LDEF craters contain both residue and the substrate material. The presence of the substrate constitutes background elemental contamination and it is highly desirable to limit or remove it from any subsequent elemental analyses. The TEM/EDX analysis of the FIB-prepared section showed that the droplet was essentially “substrate-free” with Cu from the TEM grid as the only extraneous peak observed in the spectrum (Fig. 4).

Previous studies of residue chemistry preserved in craters have involved mapping techniques, such as EDX or SIMS (e.g. Bunch et al., 1991; Bernhard et al., 1993; Graham et al., 2000). However, unless the impact features are particularly shallow in depth, there will be a significant issue with regards to the exposure of the interior surface of the crater to the instrument detector due to geometry. The effect of this is an incomplete line-of-sight of emitted x-rays or ions to the detector resulting in typically only the rims of the crater showing the location of residue material (e.g. Fig. 1 and Stephan et al., 2005). In addition, instruments such as the NanoSIMS have very specific geometric requirements for sample preparation with specimen height and topography being critical factors. The ability to prepare electron transparent sections of either individual melt residue as

discussed herein or entire cross-sections of micro-craters (Leroux et al., 2005) maximizes the potential of coordinated studies. It has previously been shown from recent integrated studies of IDPs that a single FIB section can be investigated using multiple techniques to gain mineralogical, chemical and isotopic information, and the same approach will be applied to Stardust samples (Floss et al., 2004; Bradley et al., 2005).

Conclusion

Cometary material from a known source is a significant addition to the current repository of extraterrestrial materials available for laboratory studies. However the ability to interpret the nature of the materials will depend on the level of micro-analytical characterization that can be performed. Whether it is particles embedded in aerogel or residue fused to the walls of micro-craters, the captured cometary debris must be liberated from the collection substrate. While FIB microscopy is not the only method available to recover material, it is the only one that can be demonstrated to work at the spatial resolution suitable for material generated by hypervelocity particle collisions in nonporous targets

Acknowledgments

This work was in part performed under the auspices of the U.S. Department of Energy, National Nuclear Security Administration by the University of California and Lawrence Livermore National Laboratory under contract no. W-7405-Eng-48. This work was in part supported by NASA grant NNH04AB49I to John Bradley and by Stardust Project funds to Friedrich Hörz.

References

Bernhard R.P., See T.H., and Hörz F. 1993. Projectile compositions and modal frequencies on the “Chemistry of micrometeoroids” LDEF experiment. In *LDEF – 69 months in Space Second Post-Retrieval Symposium*, NASA CP-3194 Part 2. pp551-573.

Bradley J., Dai Z.R., Erni R., Browning N., Graham G., Weber P., Smith J., Hutcheon I., Ishii H., Bajt S., Floss C., Stadermann F., and Sandford S. 2005. An astronomical 2175 Å feature in interplanetary dust particles. *Science* 307: 244-247.

Bradley J.P., Keller L.P., Snow T.P., Hanner M.S., Flynn G.J., Gezo J.C., Clemett S.J., Brownlee D.E., and Bowey J.E. 1999. An infrared spectral match between GEMS and interstellar grains. *Science* 285: 1716-1718.

Bradley J.P., and Brownlee D.E. 1986. Cometary particles: Thin sectioning and electron beam analysis. *Science* 231: 1542-1544.

Bradley J., Carey W., and Walker R.M. 1986. Solar Max impact particles: perturbation of captured material. 17th Lunar and Planetary Science Conference. pp81-82.

Brownlee D.E. 2003. Comets. In *Meteorites, Comets, and Planets*, Treatise on Geochemistry Vo.1, edited by Davis A.M., executive editors Holland H.D and Turekian K.K. Amsterdam: Elsevier B.V. pp663-688.

Brownlee D.E., Hörz F., Newburn R.L., Zolensky M., Duxbury T.C., Sandford S., Sekanina Z., Tsou P., Hanner M.S., Clark B.C., Green S.F., and Kissel J. 2004. Surface of a young Jupiter family comet 81P/Wild-2: View from the Stardust spacecraft. *Science* 304: 1764-1769.

Brownlee D.E., Tsou P., Anderson J.D., Hanner M.S., Newburn R.L., Sekanina Z., Clark B.C., Hörz F., Zolensky M.E., Kissel J., McDonnell J.A.M., Sandford S.A., and Tuzzolino A.J. 2003. Stardust: Comet and interstellar dust sample return mission. *Journal of Geophysical Research* 108 (E10): 8111.

Bunch T.E., Radicati di Brozolo F., Fleming R.H., Harris D.W., Brownlee D., and Reilly T.W. 1991. LDEF impact craters formed by carbon-rich impactors: A preliminary report. In *LDEF – 69 months in Space First Post-Retrieval Symposium*, NASA CP-3134 Part 1. pp549-564

Floss C., Stadermann F.J., Bradley J., Dai Z.R., Bajt S., and Graham G. 2004. Carbon and nitrogen isotopic anomalies in an anhydrous interplanetary dust particle. *Science* 303: 1355-1358.

Graham G.A., Grant P.G., Chater, R.J., Westphal A.J., Kearsley A.T., Snead C., Dominguez G., Butterworth A.L., McPhail D.S., Bench G., and Bradley J.P. 2004. Investigation of ion beam techniques for the analysis and exposure of particles

encapsulated by silica aeogel: applicability for Stardust. *Meteoritics and Planetary Science* 39: 1461-1473.

Graham G.A., Kearsley A.T., Grady M.M., Wright I.P., and McDonnell J.A.M. 2000. The collection of micrometeoroid remnants from low Earth orbit. *Advances in Space Research* 25: 303-307.

Hanner M.S. 2003. The mineralogy of cometary dust. In, *Astromineralogy*, Lecture Notes in Physics 609, edited by Henning Th. Berlin Heidelberg New York: Springer. pp 171-188.

Ishii H.A., Graham G.A., Kearsley A.T., Grant P.G., Snead C.J., and Bradley, J.P. 2005a. Ultrasonic micro-blades for the rapid extraction of impact tracks from aerogel (abstract #1387), 36th Lunar and Planetary Science Conference. CD-ROM.

Ishii H.A., Brennan S., Luening K., Pianetta, P., Bradley J.P., Snead C.J., and Westphal A.J. 2005b. Hard x-ray spectro-microscopy techniques at SSRL for astromaterials analysis (abstract #1393). 36th Lunar and Planetary Science Conference. CD-ROM.

Kearsley A.T., Burchell M.J., Hörz F., Cole M., and Schwandt C.S. 2006. Laboratory simulation of impacts upon metallic foils of the Stardust spacecraft: Calibration of dust particle size from comet Wild2. *Meteoritic and Planetary Science*. This volume

Kearsley A.T., Drolshagen G., McDonnell J.A.M., Mandeville J.-C., and Moussi A. 2005. Impacts on Hubble Space Telescope solar arrays: discrimination between natural and man-made particles. *Advances in Space Research* 35: 1254-1262

Kissel J., Brownlee D.E., Büchler K. Clark B.C., Fechtig H., Grün E., Hornung K., Igenbergs E.B., Jessberger E.K., Krueger F.R., Kuczera H., McDonnell J.A.M., Morfill G.M., Rahe J., Schwehm G., Sekanina, Utterback N.G., Völk H.J., and Zook H.A. 1986. Composition of comet Halley dust particles from Giotto observations. *Nature* 321: 336-337.

Kissel J., Krueger F.R., Silén J., and Clark B.C. 2004. The cometary and interstellar dust analyzer at comet 81P/Wild 2. *Science* 304: 1774-1776.

Leroux H., Borg J., Troadec D., Djouadi Z. and Hörz F. 2006. Microstructural study of micron-sized craters simulating Stardust impacts in aluminum 1100 targets. *Meteoritics and Planetary Science*. This volume.

Phaneuf M.W. 2004. FIB for material science applications – A review. In *Introduction to focused ion beams – instrumentation, theory, techniques and practice*, edited by Giannuzzi L.A., and Stevie F.A. New York: Springer. pp 143-172.

Teetsov A., and Bradley J. 1986. Micromanipulation of extraterrestrial particles. 17th Lunar and Planetary Science Conference. pp 883-884

Tsou P., Brownlee D.E., Sandford S.A., Hörz F., and Zolensky M.E. 2003. Wild 2 and interstellar sample collection and Earth return. *Journal of Geophysical Research* 108 (E10): 8113.

Tuzzolino A.J., Economou T.E., Clark B.C., Tsou P., Brownlee D.E., Green S.F., McDonnell J.A.M., McBride N., Colwell M.T.S.H. 2004. Dust measurements in the coma of comet 81P/Wild 2 by the dust flux monitor instrument. *Science* 304: 1776-1780.

Stephan T., Leitner J., and Hörz F. 2005. TOF-SIMS analysis of residues from Allende projectiles shot onto aluminum foil – A Stardust dress rehearsal (abstract #4034). Workshop on dust in planetary systems. LPI contribution No.1280. Houston: Lunar and Planetary Institute. CD-ROM.

Westphal, A.J., Snead, C., Butterworth, A., Graham, G.A., Bradley, J.P., Bajt, S., Grant, P.G., Bench, G., Brennan, S., Pianetta, P. 2004. Aerogel keystones: Extraction of complete hypervelocity impact events from aerogel collectors. *Meteoritics and Planetary Science* 39: 1375-1386.

Zolensky M.E., Pieters C., Clark B., and Papike J.J. 2000. Small is beautiful: The analysis of nanogram-sized astromaterials. *Meteoritics and Planetary Science* **35**: 9-29.

Figure Captions

Fig. 1. a) Secondary electron image of an impact crater generated by a nominal 49 μm projectile at 6.35 km/s that has completely penetrated the 100 μm thick foil. b) A typical X-ray energy-dispersive spectrum (EDS) acquired for the residue material preserved on the rim of the crater. There is significant contribution of Al foil substrate detected in the spectrum. c) X-ray EDS map for Si locating the distribution of the projectile residue on the crater lip. d) X-ray EDS map for Na corresponding with the Si map. e) Overlay composite map for Al (substrate) against Na and Si (soda lime glass residue).

Fig. 2. a) Secondary electron image of an impact feature. b) Ion-induced secondary electron image of the same feature. Extraneous residue material is clearly identified on the walls and rim of the crater due to enhanced material contrast.

Fig. 3. Secondary electron images showing the extraction and subsequent thinning of a residue droplet from the interior wall of an impact penetration. a) The impact penetration containing the melt droplet (see the white arrow marker). b) The melt droplet prior to ion milling. c) High precision FIB milling was then used to remove the bulk of the material attaching the droplet to the crater wall. d) The in-situ extraction of the droplet from the crater wall using the OmniprobeTM tungsten needle nanomanipulator. e) The droplet welded to the copper TEM grid prior to ion thinning, using the FIB, to electron transparency thickness. f) The droplet after final thinning.

Fig. 4. a) Bright-field TEM image of melt droplet. c) X-ray EDS acquired from the core of the droplet. Note, after removing the droplet from the crater wall, the significant Al peak observed in Figure 1b is now absent. Also there is no evidence of Ga in the spectrum that might have been implanted during the FIB milling. The only extraneous elemental peak observed in the spectrum is Cu from the TEM grid.

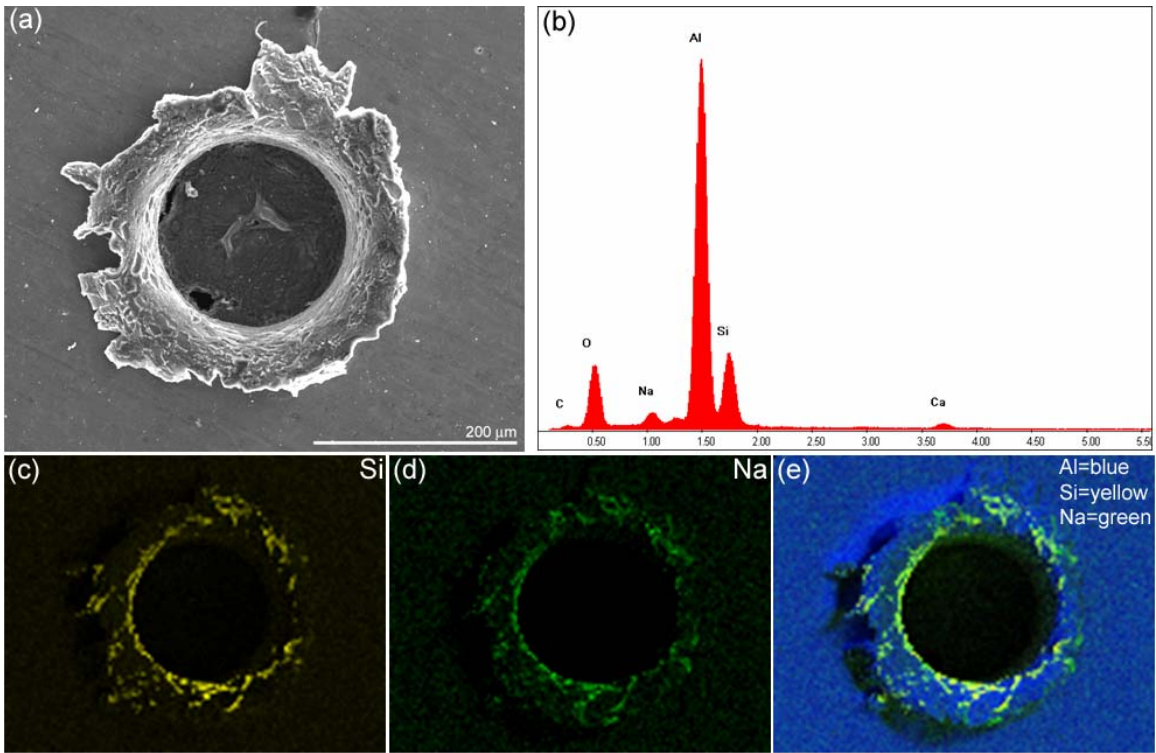


Fig. 1.

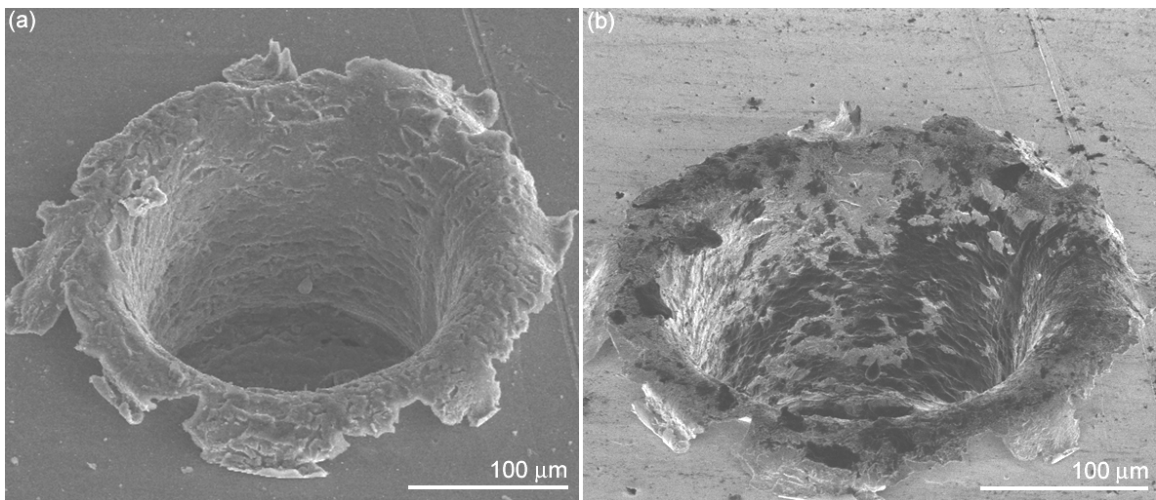


Fig. 2.

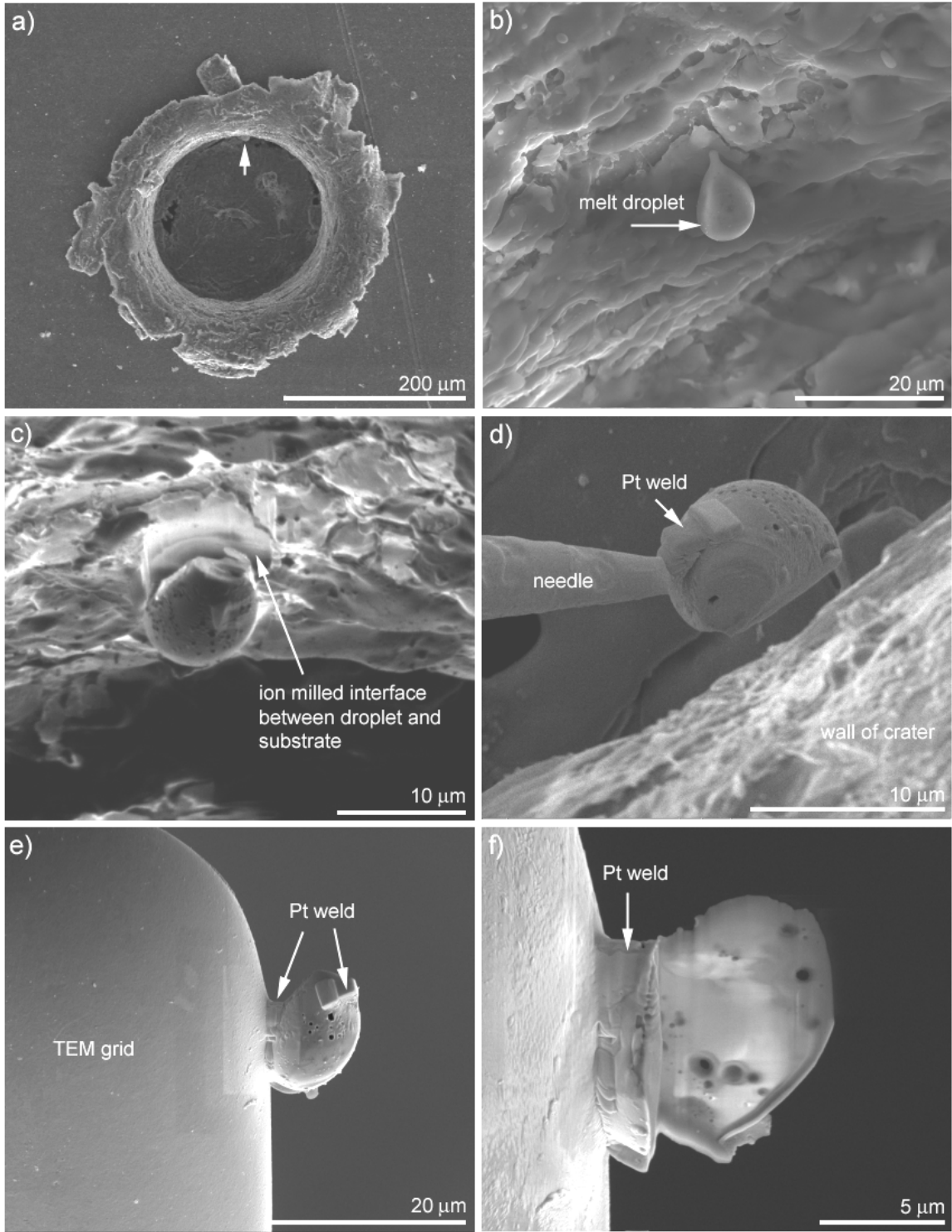


Fig. 3.

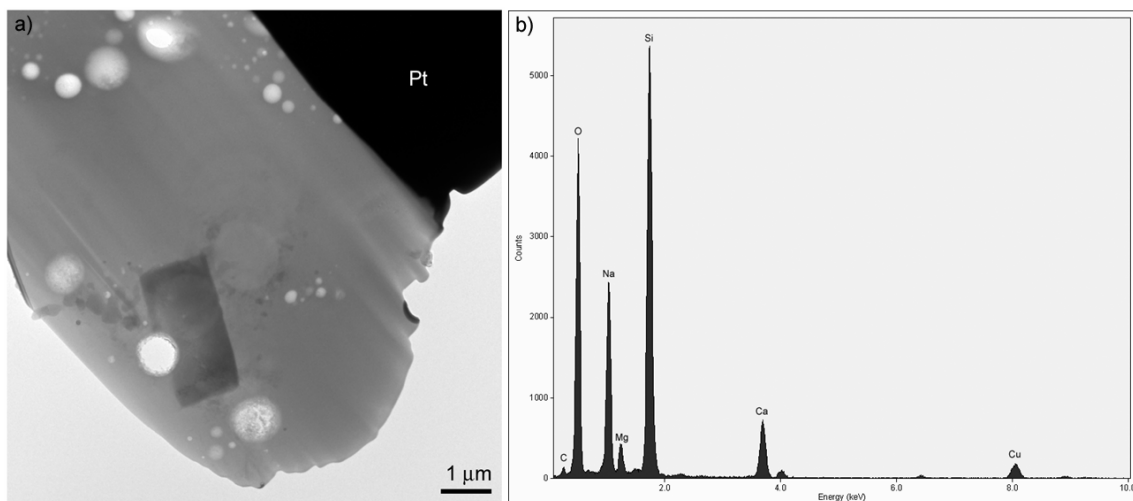


Fig. 4.